

# FTIR ATR Studies on Immobilized Mitochondrial Creatine Kinase

M.Siam\*, D. Baurecht\*, G.Reiter\*, U.Schlattner#, T. Wallimann# and U.P. Fringeli\*  
 \*Institute of Physical Chemistry, University of Vienna, Althanstrasse 14, A-1090 Vienna, Austria  
 #Institute for Cell Biology, ETH Hönggerberg, Zürich, Switzerland



## INTRODUCTION

Fourier Transform Infrared Attenuated Total Reflexion (FTIR ATR) spectroscopy provides an appropriate tool to investigate interactions between membrane proteins and lipid bilayers mimicking a biological membrane. Its great advantages are a high sensitivity even in aqueous systems and, using polarized light, the access to informations about the structural order within the membranes. With the set up shown in Fig. 1 it is possible to observe interactions between reagents and components of the membrane *in situ* [1]. Furthermore, a chopper behind the cuvette splits the beam and allows one to measure sample and reference spectra quasi simultaneously (single beam sample reference (SBSR)-technique).

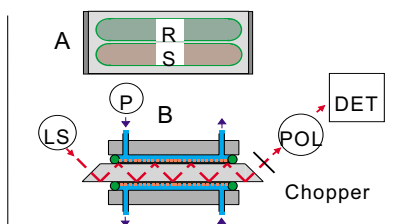


Fig. 1: Single beam sample reference (SBSR) arrangement for a flow through cuvette with two compartments. A) The Ge plate functioning as multiple internal reflection element (MIRE) and support for the membranes is divided into a sample (S) and the reference (R) compartment by the sealing of the cuvette. B) A parallel incident beam from the light source (LS) is focused on the entrance face of the Ge plate. Every reflection is accompanied by absorptions of the membrane and the bulk. A chopper divides the single beam into a sample S and a reference R beam before they pass a polarisator (POL) and impinge on the detector (DET). Solutions and buffers are moved through the compartments by the means of a peristaltic pump (P).

*In vivo* mitochondrial creatine kinase (Mi-CK) is found in the intermembrane space, attached to the inner mitochondrial membranes, which are rich of the negatively charged cardiolipin (CL) [2]. Through phosphorylation from phosphocreatin (PCr) to ADP producing ATP (or *vice versa*) the enzyme realizes a temporal and spatial energy buffering. The native form is octameric and shaped as a cube with a canal in the middle, as revealed by x-ray diffraction [3]. Two opposite faces are enriched of Lys and Arg, enabling the attachment to negatively charged bilayers. Two types of bilayers, either of dipalmitin phosphatidic acid (DPPA) solely or of DPPA and CL, were offered for immobilization.

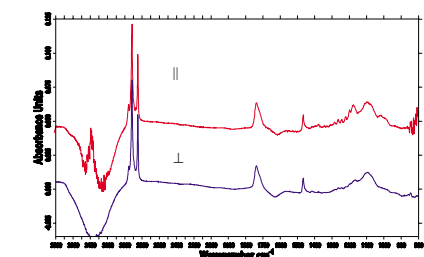


Fig. 2: Parallel (||) and vertical (⊥) polarized IR ATR absorbance spectra of a DPPA bilayer. DPPA bilayer transferred from an aqueous subphase ( $10^{-4}$  M CaCl<sub>2</sub>) to a germanium plate at 30mN/m with 2 mm/min; 20 mM phosphate buffer pH 7.0, T 25°C; reference: Ge plate and 20 mM phosphate buffer pH 7.0, T 25°C;  $\Gamma = 3.1 \cdot 10^{-10}$  mol·cm<sup>-2</sup>; dichroic ratio R ( $A_{\parallel}/A_{\perp}$ ) = 0.92; angle of incidence 45°; number of active internal reflections N = 28.0.

## MATERIALS AND METHODS

**Preparation of bilayers.** DPPA was transferred at 30 mN/m to the Ge plate with the Langmuir-Blodgett (LB)-methode, either one for the CL/DPPA bilayers or two for the DPPA bilayers. The second leaflet of the CL/DPPA bilayers was built up by using the spontaneous adsorption of CL from a vesicle solution (LB/vesicle-methode) [4]. Fig. 3 visualizes the stepwise preparation, whereby step by step spectra like Fig. 2 and Fig 4 can be used to characterize and quantify the results.

**Activity control measurements.** The activity was verified *in situ* by observing the decrease of typical PCr and ADP IR signals when a substrate solution with 20mM PCr and 4mM ADP is pumped through the cuvette. The SBSR absorbance spectra (S-R) display directly the amount of turnover to Cr and ATP.

**Interaction with MgADP.** 10mM MgADP in 20mM D<sub>2</sub>O phosphate buffer pH 7.0 was flushed through both compartments of the cuvette. The SBSR technique records the enzyme-MgADP complex and compensates the MgADP signal (Fig.6)

**Adsorption of Mi-CK on bilayers and Ge.** The clean Ge plate resp. the bilayers were exposed to 0.6 mg/ml enzyme solution and the adsorption process was monitored. Afterwards the solution was replaced by buffer and spectra of the immobilized enzyme were measured.

**HD exchange of Mi-CK adsorbed on bilayers.** D<sub>2</sub>O phosphate buffer was pumped into the cuvette and the shift from amide II to amide II' was observed for several hours. HDO compensation was achieved through the SBSR arrangement.

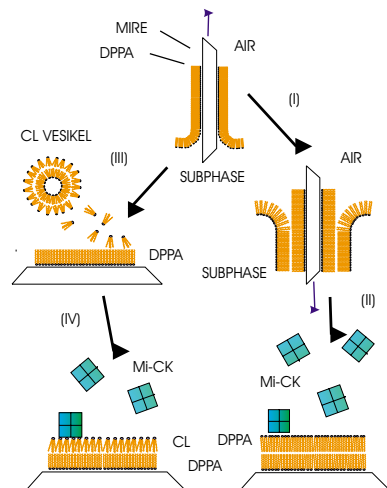


Fig. 3: Schematic description of the two pathways to build up the bilayers used for immobilization of Mi-CK. Both paths start with the transfer of a DPPA monolayer from the air/water interface of a film balance to the Ge plate by the Langmuir-Blodgett (LB) technique. Path 1: The second leaflet is deposited by dipping the plate into the subphase again (I). During every step of further handling contact to air was avoided to assure an intact bilayer for protein adsorption (II). Path 2: (III) Due to hydrophobic interactions CL adsorption occurred from a vesicle solution spontaneously resulting in an asymmetric bilayer mimicking the mitochondrial membrane. This bilayer was offered to the Mi-CK (IV).

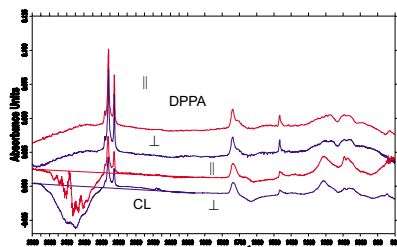


Fig. 4: Polarized IR ATR absorbance spectra of DPPA and CL constituting a bilayer. Top: DPPA monolayer transferred from an aqueous subphase ( $10^{-4}$  M CaCl<sub>2</sub>) to a germanium plate; spectra were measured against air. Surface concentration was calculated with the thin film approximation:  $\Gamma = 3.10^{-10}$  mol·cm<sup>-2</sup>, dichroic ratio R ( $A_{\parallel}/A_{\perp}$ ) = 0.93; angle of incidence 45°; number of active internal reflections N = 40.7. Bottom: CL from *E. Coli* assembled from a vesicle solution (0.7mg/ml) on the DPPA monolayer. This bilayer was in contact with 20 mM phosphate buffer pH 7.0, T 18°C; reference: DPPA in 20 mM phosphate buffer pH 7.0; surface concentration  $\Gamma = 1.7 \cdot 10^{-10}$  mol·cm<sup>-2</sup>; dichroic ratio R ( $A_{\parallel}/A_{\perp}$ ) = 1.16; angle of incidence 45°; number of active internal reflections N = 16.2.

## RESULTS AND DISCUSSION

**Adsorption of Mi-CK on bilayers and Ge.** Beside the immobilization of Mi-CK to the negatively charged bilayers, adsorption to Ge was found, too. Evidently from data of Tab.1, adsorption to the DPPA bilayer ends up in the greatest density of coverage and with the smallest dichroic ratio R for the protein. Compared to the CL/DPPA bilayer, the DPPA bilayer opposes a higher charge density, as can be revealed by a smaller R evolving from a higher order within the DPPA bilayer. This results in a higher protein coverage with better order strongly supporting electrostatic attraction between Lys and Arg and the lipid headgroups as driving force for the adsorption process. Adsorption of Mi-CK to the DPPA bilayers does not change their dichroic ratio for vCH stretch indicating that the enzyme is not penetrating and disturbing the DPPA leaflet. Dichroic ratios for vCH stretch of the CL layer increase after adsorption of Mi-CK. The enzyme seems to sink into the more elastic CL leaflet.

### REFERENCES

- [1] Fringeli, U. P., Goette, J., Reiter, G., Siam, M. and Baurecht, D., *Proceedings of the 11th International Conference on Fourier Transform Spectroscopy*, James A. de Haseth, Ed., AIP Conference Proceedings no. 430, (1998). The American Institute of Physics, Woodbury, NY.
- [2] Wallimann, T., Wyss, M., Brdiczka, D., Nicolay, K. and Eppenberger, H.M. *Biochem. J.* 281, 21-40 (1992).
- [3] Fritz-Wolf, K., Schnyder, T., Wallimann T. and Kabsch, W., *Nature* 381, 341-345 (1996).
- [4] Wenzl, P., Fringeli, M., Goette, J. and Fringeli, U. P., *Langmuir* 10, 4253-4254 (1994).
- [5] Raimbault, C., Buchet, R. and Vial, C., *Eur. J. Biochem.* 240, 134-142 (1996).

**HD exchange of the system.** The amide II (1550cm<sup>-1</sup>), the amide II' (1450cm<sup>-1</sup>) and the NH stretching (3300cm<sup>-1</sup>) bands can be used to analyse the flexibility of the protein. The octameric 645kD Mi-CK is a rather stiff protein and/or possesses inaccessible regions. About 30% of the amide protons are hardly exchanged at all within the duration of experiment of 20 hours (Fig.5).

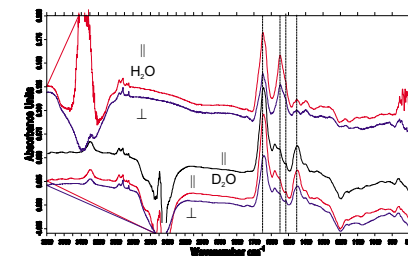


Fig. 5: Polarized IR ATR absorbance spectra of immobilized Mi-CK during the HD exchange. Protein adsorbed from 0.6 mg/ml solution to a DPPA bilayer. Top: H<sub>2</sub>O SBSR absorbance spectra (S-R) S: Mi-CK on DPPA; R: DPPA bilayer; both in 20 mM phosphate buffer pH 7.0, T 25°C; Middle: D<sub>2</sub>O SBSR absorbance spectra (S-R) after 2h; Bottom: D<sub>2</sub>O SBSR absorbance spectra (S-R) after 17h; both compartments with 20 mM phosphate buffer pH 6.6, T 25°C;  $\Gamma = 1.10^{-10}$  mol·cm<sup>-2</sup>; dichroic ratio R ( $A_{\parallel}/A_{\perp}$ ) = 1.7; angle of incidence 45°; number of active internal reflections N = 24.47; amid I, amid II, tyrosin (ν C-C ring) and amide II' band are marked with lines.

**Activity control measurements** revealed activity loss but proved the preservation of 50% of the initial activity after 115 hours.

**Interaction with MgADP.** The difference SBSR absorbance spectra shown in Fig. 6 reflect the alterations through binding of MgADP to Mi-CK in protein structure and for aminoacid sidechains involved. The prominent peaks at 1652 cm<sup>-1</sup> (α-helix) and 1637 cm<sup>-1</sup> (β-helix) can be assigned to changes of the secondary structure. Whereas the peaks at 1606 cm<sup>-1</sup>, 1585 cm<sup>-1</sup>, 1569 cm<sup>-1</sup> and 1518 cm<sup>-1</sup> can be related to sidechain absorption of Arg, Asp, Glu and Tyr. The peak at 1627 cm<sup>-1</sup> reflects changing H-bridges of Asp and Glu [5]. Polarization for the band at 1652 cm<sup>-1</sup> indicates that an α-helix, with the transition moment rather parallel to the bilayer surface, takes part in the binding of the Mi-CK/MgADP-complex. Data from Lit. [5] are derived from FTIR difference spectra produced with the help of caged substrates. Their photoproducts may interact with the enzyme and it can be sophisticated to separate these effects from the substrate-enzyme binding.

FTIR ATR and the SBSR technique provide an elegant access to investigation of structure-function relationships like the binding studies of MgADP to Mi-CK.

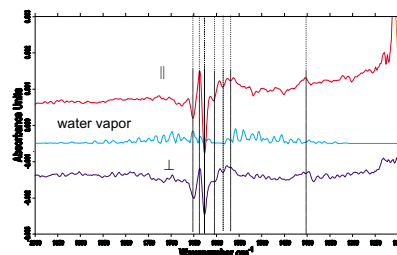


Fig. 6: Difference of SBSR absorbance spectra [Mi-CK/MgADP]-[Mi-CK] parallel (||) and vertical (⊥) polarized. S: Mi-CK on DPPA bilayer;  $\Gamma = 0.7 \cdot 10^{-10}$  mol·cm<sup>-2</sup>; R: DPPA bilayer; for both compartments the bulk was 10 mM MgADP in D<sub>2</sub>O phosphate buffer pH 6.6. The lines mark peaks at 1652 cm<sup>-1</sup>, 1637 cm<sup>-1</sup>, 1627 cm<sup>-1</sup>, 1607 cm<sup>-1</sup>, 1586 cm<sup>-1</sup>, 1569 cm<sup>-1</sup>, 1586 cm<sup>-1</sup>, 1518 cm<sup>-1</sup> and 1403 cm<sup>-1</sup>, and relate them to the water vapor spectra in the middle.

Tab.1: Results of Mi-CK adsorption from a 0.6 mg/ml solution to three types of surfaces. The bilayers and the proteinlayer are characterized by the surface concentration (Γ) and the dichroic ratio R. Surface concentration was calculated with the thin film approximation (angle of incidence θ = 45°). For the lipids the mean head group area (A) and for the protein the mean side length (a) is listed.

| surface         | surface characterization                  |      |                            | characterization of immobilized Mi-CK     |      |              |                      |
|-----------------|---|------|----------------------------|---|------|--------------|----------------------|
|                 | Γ   | R    | A                          | Γ   | R    | a            | protein coverage (%) |
|                 | [10 <sup>-10</sup> mol·cm <sup>-2</sup> ] |      | [Å <sup>2</sup> /molecule] | [10 <sup>-10</sup> mol·cm <sup>-2</sup> ] |      | [Å/molecule] |                      |
| Ge              | -   | -    | -                          | 1.01                                      | 1.72 | 128          | 53                   |
| DPPA bilayer    | 3.1                                       | 0.92 | 55                         | 1.40                                      | 1.63 | 109          | 73                   |
| DPPA/CL bilayer | -   | -    | -                          | 1.05                                      | 1.65 | 126          | 55                   |
| DPPA            | 3.2                                       | 0.93 | 52                         | -   | -    | -            | -                    |
| CL              | 1.7                                       | 1.16 | 99                         | -   | -    | -            | -                    |

### ACKNOWLEDGEMENTS

Grant No. 5730 by the Jubiläumsfonds of the Oesterreichische Nationalbank is kindly acknowledged. It enabled scholarship to M.S. M.S wish to thank M. Riesing for assistance and discussion.

Correspondence: Monira Siam (siam@ftp.bpc.univie.ac.at)